

## **Quantifying the area-at-risk in reperfused STEMI patients using hybrid cardiac PET-MR imaging**

Heerajnarain Bulluck MBBS\*<sup>1,2</sup>, Steven K White BSc MBChB\*<sup>1,2</sup>,  
Georg M Fröhlich MD<sup>2</sup>, Steven G Casson MA MB BChir MSc<sup>3</sup>, Celia O'Meara BSc<sup>4</sup>,  
Ayla Newton BSc<sup>1</sup>, Jennifer Nicholas PhD<sup>5</sup>, Peter Weale BA DCR(R)<sup>6</sup>,  
Simon MY Wan MD<sup>4</sup>, Alex Sirker PhD<sup>2</sup>, James C Moon MD<sup>2</sup>, Derek M Yellon DSc  
PhD<sup>1,2</sup>, Ashley Groves MD PhD<sup>4</sup>, Leon Menezes BM BCh<sup>4</sup>,  
Derek J Hausenloy MD PhD<sup>1,2,7,8</sup>

### **\*Joint first authors**

<sup>1</sup>The Hatter Cardiovascular Institute, Institute of Cardiovascular Science, University College London, UK

<sup>2</sup>The National Institute of Health Research University College London Hospitals Biomedical Research Centre, UK

<sup>3</sup>Independent researcher

<sup>4</sup>UCL Institute of Nuclear Medicine, University College London Hospital, UK.

<sup>5</sup>London School Hygiene and Tropical Medicine, London, UK

<sup>6</sup>Siemens Healthcare, Frimley, UK.

<sup>7</sup>Cardiovascular and Metabolic Disorders Program, Duke-National University of Singapore

<sup>8</sup>National Heart Research Institute Singapore, National Heart Centre Singapore

**Short running title:** Hybrid PET-MR imaging of the AAR in STEMI

### **Corresponding author:**

Dr Steven K. White

The Hatter Cardiovascular Institute, Institute of Cardiovascular Science,  
NIHR University College London Hospitals Biomedical Research Centre,  
University College London Hospital & Medical School,  
67 Chenies Mews, London,  
WC1E 6HX, UK.

Tel: +44 (203) 447 9888

Fax: +44 (203) 447 9505

E-mail: [stevenkwhite@gmail.com](mailto:stevenkwhite@gmail.com)

## **Abstract**

**Background:** Hybrid Positron Emission Tomography and Magnetic Resonance (PET-MR) allows the advantages of MR in tissue characterizing the myocardium to be combined with the unique metabolic insights of PET. We hypothesized that the area of reduced myocardial glucose uptake would closely match the area-at-risk (AAR) delineated by T2-mapping in ST-segment elevation myocardial infarction (STEMI) patients.

**Methods and results:** Hybrid PET-MR using  $^{18}\text{F}$ -fluorodeoxyglucose (FDG) for glucose uptake was performed in 21 STEMI patients at a median of 5 days. Follow-up scans were performed in a subset of patients 12 months later. The area of reduced FDG uptake was significantly larger than the infarct size quantified by late gadolinium enhancement (LGE) ( $37.2\pm 11.6\%$  versus  $22.3\pm 11.7\%$ ;  $P<0.001$ ), and closely matched the AAR by T2-mapping ( $37.2\pm 11.6\%$  versus  $36.3\pm 12.2\%$ ;  $P=0.10$ ,  $R=0.98$ , bias  $0.9\pm 4.4\%$ ). In the follow-up scans, the area of reduced FDG uptake was significantly smaller in size when compared to the acute scans ( $19.5 [6.3-31.8]\%$  versus  $44.0 [21.3-55.3]\%$ ,  $P=0.002$ ), and closely correlated with the areas of LGE ( $R=0.98$ ) with a small bias of  $2.0\pm 5.6\%$ . An FDG uptake of  $\geq 45\%$  on the acute scans could predict viable myocardium on the follow-up scan. Both transmural extent of LGE and FDG uptake on the acute scan performed equally well to predict segmental wall motion recovery.

**Conclusions:** Hybrid PET-MR in the reperfused STEMI patient showed reduced myocardial glucose uptake within the AAR and closely matched the AAR delineated by T2-mapping. FDG uptake, as well as transmural extent of LGE acutely can identify viable myocardial segments.

**KEYWORDS:** Hybrid PET-MR imaging, ST-segment elevation myocardial infarction, T2-mapping, area-at-risk, <sup>18</sup>F-fluorodeoxyglucose

## **INTRODUCTION**

In the first few days following an acute ST-segment elevation myocardial infarction (STEMI), cardiac magnetic resonance (MR) imaging can assess regional/global left ventricular function, myocardial infarct (MI) size, the 'area-at-risk' (AAR)<sup>1, 2</sup>, the presence of microvascular obstruction (MVO)<sup>3</sup> and intra-myocardial hemorrhage<sup>4</sup> - features which not only provide important prognostic information but may also serve as surrogate endpoints in cardioprotection studies. These omit a key biological parameter, cardiac metabolism, currently inaccessible by conventional MR imaging.

The recent availability of hybrid Positron Emission Tomography and Magnetic Resonance (PET-MR) imaging offers the unique advantage of simultaneous tissue characterization by MR to be combined with the metabolic insights provided by PET, without requiring an acutely unwell patient to undergo two separate scans, and obviating complex and potentially imprecise co-registration of separately acquired PET and MR datasets. To date, there has been limited experience with hybrid PET-MR imaging of the heart<sup>5-8</sup>. T2-weighted MR imaging of myocardial edema has been used to quantify the AAR in STEMI patients, a pre-requisite for calculating myocardial salvage - a critical measure of efficacy in cardioprotection studies<sup>1, 9, 10</sup>. Hybrid PET-MR imaging of the reperfused heart therefore, provides the opportunity to investigate cardiac metabolism in salvaged, reversibly injured myocardium within the AAR. The area of reduced myocardial glucose uptake has recently been shown to overestimate the AAR assessed by endocardial surface area (ESA).<sup>11</sup> We hypothesized that the area of reduced myocardial glucose uptake would closely match the area-at-risk (AAR) delineated by T2-mapping in STEMI patients treated by PPCI.

## **METHODS**

### **Study population**

We performed a single-center study of 22 STEMI patients treated by PPCI recruited over a 7-month period. Study exclusion criteria were as follows:  $\leq 45$  years of age (to attenuate any theoretical higher risk from ionizing radiation in younger patients); diabetes mellitus (as pre-existing metabolic/glycemic derangement may affect clarity of initial results); previous MI; and standard recognized contraindications to MR. All eligible patients provided informed and written consent. The study was approved by the UK National Research Ethics Service.

### **Hybrid PET-MR cardiac imaging protocol**

Patients underwent hybrid PET-MR imaging at a median of 5 [4-6] days after PPCI using an integrated whole-body PET-MR (3.0 Tesla) scanner (Biograph mMR, Siemens Healthcare, Erlangen, Germany)(Figure 1). A subset of patients underwent a follow-up scan at 12 months.  $^{18}\text{F}$ -fluorodeoxyglucose (FDG) was used to assess resting myocardial glucose metabolism. Subjects fasted for a minimum of 6 hours followed by 75g of oral glucose 2 hours prior to the scan, and 45-60 minutes later, insulin was administered as previously described<sup>12</sup>, followed by intravenous FDG (mean activity of  $248 \pm 15$  MBq) at a mean of  $73 \pm 12$  minutes prior to PET images acquisition.

A standard cardiac MR imaging protocol<sup>13</sup> including cine imaging, and T2-mapping and late gadolinium enhancement (LGE) imaging performed simultaneously with the FDG-PET acquisition following single breath-hold attenuation correction (AC). LGE imaging was performed using a standard segmented 'fast low-angle shot' two-dimensional inversion-recovery gradient echo sequence 10-15 minutes after the injection of Gadoterate meglumine (Gd-DOTA marketed as Dotarem, Guerbet S.A.,

Paris, France) at a dose of 0.1 mmol/kg and T2 maps (Works in Progress, software WIP #699, Siemens Healthcare, Frimley, UK) were acquired as previously described<sup>14</sup>. In brief, 3 single-shot images at different T2 preparation times (0ms, 24ms, and 55ms, respectively) using the following parameters were acquired: repetition time=3xR-R interval; acquisition matrix=116x192; flip angle=65°; slice thickness=6mm with 4mm gap; field of view adjusted according to subject size (320-400mm). Motion correction and fitting were performed to estimate coefficients of the decay function, which was subsequently used to estimate T2 relaxation times. An in-built specific color look-up table was used to output the final color T2 maps, consisting of pixel-wise T2 values. A full stack of short axis slices was acquired to cover the left ventricular (LV) from base to apex – each MR modality matching exactly the same slice position.

FDG-PET images were acquired with one bed position, gated by electrocardiography, and comprised three-dimensional isotropic image reconstruction (voxel size, 2x2x2 mm<sup>3</sup>) using Poisson ordered-subset expectation maximization with 21 subsets and three iterations, a Gaussian filter with 5.0-mm full-width at half maximum, and a 344x344 image matrix to obtain summed average FDG-PET images. A four-compartment model PET attenuation map was calculated using the MR capabilities of the machine using fat-only and water-only Dixon-based sequences for automatic PET AC<sup>15</sup>.

## **Image analysis**

### *Co-localization of the MI territory with FDG uptake*

Co-localization of the MI territory with FDG uptake was evaluated using ‘fused’ FDG-LGE images created by fusing individual end-diastolic LGE short-axis slices with the summed static FDG-PET images using OsiriX freeware (Version 5.8.5, Geneva,

Switzerland). The fused images were then visually assessed to identify areas of LGE and reduced FDG uptake.

#### *Quantification of AAR, MI size and FDG uptake*

Quantification of LV volumes, LV mass, LV ejection fraction, AAR by T2-mapping, regions of reduced FDG uptake and MI size were performed using CVI<sup>42</sup> software (Version 5.1.0, Calgary, Canada). As described above, each end-diastolic LGE slice was initially fused with the summed static FDG-PET images, extracting both a fused and a sliced-matched non-fused FDG image. These non-fused FDG LV short axis slices, along with their corresponding T2 maps were used for quantification. The epicardial and endocardial borders were first manually traced on the T2 maps and LGE images and copied onto the FDG images with minimal manual adjustment. The MI size was quantified by the Otsu-auto-thresholding (OAT) technique. Two blinded operators independently analyzed the T2 maps (OAT) and FDG-PET images (manual delineation of the regions with reduced FDG uptake on the summed images with visual optimization of the window settings by 2 operators). Areas of MVO were included as part of the MI and AAR on the LGE images and T2 maps, and any obvious blood pool or pericardial partial voluming and artifacts manually corrected. One operator subsequently used OAT, Full Width Half Maximum and reduction in signal intensity 2, 3, 4 and 5 standard deviations (SD) from the remote myocardium to quantify the regions of reduced FDG uptake. All of the LV short axis slices from base to apex were analyzed and the final extent of abnormal myocardium was expressed as a percentage of the LV volume. Polar maps for the FDG images were generated (Xeleris Version 3.0, GE Healthcare, Milwaukee, Wisconsin) and displayed relative segmental FDG uptake as per the AHA model, normalized to the highest signal intensity for that patient

set at 100%. A second method to quantify the reduction in FDG uptake in the infarct-related territory was also performed by using a threshold of <50% on the acute scan polar maps. A threshold of  $\geq 50\%$  on the follow-up polar maps was used for identifying viable segments.<sup>16</sup>

Segmental analysis was performed using CVI<sup>42</sup> software for early gadolinium enhancement (EGE), LGE and T2 maps and displayed according to the modified 16 segment (excluding the apex) American Heart Association (AHA) model<sup>17</sup>. The EGE images were visually analyzed by 2 experienced investigators and segments with a hypo-intense core were visually scored “0” or “1” for absence or presence of early MVO. Mean transmural extent of LGE was quantified for each short axis slice and mean segmental T2 values were also automatically generated displayed according to the modified 16 segments AHA model. Segmental wall motion analysis was visually performed by 2 experienced investigators and scored as “0” for normal; “1” for mild/moderate hypokinesis; “2” for severe hypokinesis; “3” for akinesis and “4” dyskinesis.<sup>18</sup> A reduction in segmental wall motion score of  $\geq 1$  at follow-up was defined as an improvement in segmental wall motion.

### **Coronary angiographic analysis**

Coronary angiograms were analyzed by 2 independent experienced investigators using the BARI (Bypass Angioplasty Revascularisation Investigation) and the modified APPROACH (Alberta Provincial Project for Outcome Assessment in Coronary Heart Disease) coronary angiography jeopardy scores<sup>19</sup> to provide an MR-independent estimate of the AAR.

### **Statistical analysis**

Continuous data were expressed as mean $\pm$ SD or median [interquartile range] for variables showing departure from a normal distribution. Categorical data were reported as frequencies and percentages. Intra-class correlation (ICC) coefficients for inter-observer agreement<sup>20</sup> were calculated for the T2-mapping and FDG-PET quantification by using single measures in a two-way random model for absolute agreement. Paired tests were used to compare measurements made within the same patient using 2 techniques at 1 time point (e.g. AAR by T2-mapping and FDG-PET) or using the same technique at 2 time points (e.g. reduction in FDG uptake between the acute and follow-up scans). Pearson's correlation coefficient was used to assess inter-method correlation. Bland-Altman analysis was performed to assess agreement and bias detection between methods and presented as bias $\pm$ 2SD. Variances between methods were compared using Pitman's test. Receiver Operating Characteristic (ROC) analyses were performed to assess the diagnostic performance for LGE, FDG and T2 on the acute scan for detecting viable myocardium and predicting segmental wall motion recovery. All statistical tests were two-tailed, and  $P < 0.05$  was considered statistically significant. Statistical analysis was performed using SPSS version 22 (IBM Corporation, Illinois, US). MedCalc version 15.6.1 (Medcalc Software Ostend, Belgium) was also used for ROC curve comparison using the method described by DeLong et al<sup>21</sup> and for correlation coefficient comparison described by Hinkle et al<sup>22</sup>.

## **RESULTS**

21 patients completed the full imaging protocol at a median of 5 [4-6] days (1 patient was unexpectedly claustrophobic) - 76% were male and the median time between chest pain onset and PPCI was 247 [119-687] minutes. None of the patients had left bundle

branch block. More detailed patients characteristics and coronary angiographic details are presented in Table 1. 12 patients had a follow-up scan at a median of 12 (11-14) months following PPCI.

*Area of reduced FDG uptake is larger than MI size by LGE-MR*

From the fused FDG-LGE images, 20 out of 21 patients had reduced FDG uptake in the same territory of the MI location. The area of reduced FDG uptake was significantly larger than the area of LGE ( $37.2\pm 11.6\%$  with FDG-PET versus  $22.3\pm 11.7\%$  with LGE-MR;  $P<0.001$ )(Table 2). Figures 2 and 3 show representative images of patients with a transmural MI (minimal myocardial salvage) and a subendocardial MI (significant myocardial salvage), respectively.

*Area of reduced FDG uptake delineates the AAR by T2-mapping*

There was excellent per patient inter-observer agreement for the AAR by T2-mapping and manual delineation of reduced FDG uptake, with an ICC coefficient of 0.93 (95% CI 0.83-0.97;  $P<0.001$ ) and 0.94 (95% CI 0.85-0.98;  $P<0.001$ ), respectively. Figure 4 and Table 3 show the performance of the different thresholding techniques when compared to manual delineation of the area of reduced FDG uptake. The 2 SD thresholding technique performed best with excellent correlation and agreement ( $P=0.07$ , ICC 0.99, R 0.99, bias of  $-0.9\pm 4.33\%$ ), and was used for subsequent analyses.

The area of reduced FDG uptake closely matched the AAR delineated by T2-mapping ( $37.2\pm 11.6\%$  with FDG-PET versus  $36.3\pm 12.2\%$  with T2-mapping;  $P=0.10$ ). There was an excellent correlation and agreement between the area of reduced FDG uptake and the AAR by T2-mapping (R 0.98, bias  $0.9\pm 4.4\%$ , no difference between their variances,  $P=0.28$ ) (Figure 5a and b). When using the 50% threshold on the polar

maps to quantify the area of reduced FDG uptake, there was no difference when compared with the AAR by T2-mapping ( $37.8\pm 16.9\%$  with FDG-PET versus  $36.3\pm 12.2\%$  with T2-mapping;  $P=0.10$ ). The correlation between them was 0.90 but there was a wider limit of agreement on Bland Altman analysis (bias of  $2.0\pm 15.6\%$ ). Furthermore, Pitman's test confirmed a difference in the AAR by the 2 methods ( $P<0.05$ ). For patients with an AAR of  $< 35\%$ , T2-mapping had a trend to give a higher AAR than FDG uptake whereas for an AAR of  $> 35\%$ , T2 mapping tended to be lower than FDG uptake (Figure 5c and 5d).

#### *Area of reduced FDG uptake compared to BARI and modified APPROACH scores*

The area of reduced FDG uptake correlated well with the MR-independent estimates of the AAR using the BARI and modified APPROACH coronary angiography scores but overestimated the AAR ( $37.2\pm 11.6\%$  with FDG-PET versus  $28.7\pm 8.3\%$  with BARI score,  $R 0.79$ ,  $P<0.001$  and bias of  $8.4\pm 14.2\%$  and  $37.2\pm 11.6\%$  with FDG-PET versus  $29.4\pm 9.8\%$  with APPROACH score,  $R 0.71$ ,  $P<0.001$  and bias of  $8.7\pm 17.2\%$ , respectively).

#### *Hybrid cardiac PET-MR follow-up scans*

The area of reduced FDG uptake on the follow-up scans was significantly lower than those observed on the acute scans (Median [IQR]:  $19.5 [6.3-31.8]\%$  follow-up scan versus  $44.0 [21.3-55.3]\%$  acute scan,  $P=0.002$ ), and correlated closely ( $R 0.98$ ) with the areas of LGE on the follow-up scans. The area of reduced FDG uptake was more similar to the area of LGE on the follow-up scan ( $19.5 [6.3-31.8]\%$  FDG-PET versus  $19.0 [2.0-28.0]\%$  LGE-MR,  $P=0.04$ , bias of  $2.0\pm 5.6\%$ ) (Figure 6) (Table 4). Figure 7 illustrates

the differences in FDG uptake between the acute and follow-up scans of two patients with different myocardial salvage.

#### *Reduced FDG uptake in the remote myocardium*

In one patient presenting with an acute inferior STEMI, there was an additional area of reduced FDG uptake in the remote myocardium within the non-obstructed left anterior descending (LAD) coronary artery, with the follow-up scan showing improved FDG uptake within this remote area (Figure 8). This patient was excluded from any comparison given that there was reduced FDG uptake outside of the infarct-related territory.

#### *Acute scans to assess viability*

Using an FDG uptake of  $\geq 50\%$  to indicate viable myocardium on the follow-up scan, the transmural extent of LGE on both the acute scan (AUC on the ROC curve 0.93, 95% CI 0.89 – 0.97) and the follow-up scan (AUC on the ROC curve 0.95, 95% CI 0.92 – 0.99) performed equally well at predicting viable myocardium ( $P=0.13$ ). Both acute LGE and follow-up LGE performed better than acute FDG uptake (AUC on the ROC curve 0.92, 95% CI 0.85 – 0.98) at detecting viable myocardium ( $P < 0.001$  and  $P = 0.01$  respectively for ROC curve comparison). The cut-off value of  $<50\%$  transmural LGE on the acute scan had a sensitivity of 88% and specificity of 90% and on the follow-up scan had a sensitivity of 94% and specificity of 90%. The optimal cut-off for FDG uptake on the acute scan was a value of  $\geq 45\%$ , giving a sensitivity of 85% and specificity of 95% to identify viable myocardium on follow-up. T2 performed the least well compared with LGE and FDG with an AUC of 0.79, 95% CI 0.71 – 0.87, and a cut-off value of 55ms had a sensitivity and specificity of 76%.

### *Segmental wall motion recovery*

Segmental wall motion was assessed in the 12 patients with acute and follow-up scans. 4 segments were excluded (due to incidental chronic infarct). Out of the remaining 188 segments, 94 segments (50%) had no wall motion abnormalities. The remaining 94 segments had wall motion scores as follows: (1) 20 segments; (2) 23 segments; (3) 51 segments. There was a similar correlation between wall motion score and FDG uptake on both the acute and follow-up scans (R -0.59 versus R -0.65, P 0.51).

Out of 94 segments with abnormal wall motion, 19 segments (20%) had no LGE and had lower T2 values and higher FDG uptake than the 75 segments (80%) with the presence of LGE (T2: 48.9±5.1ms versus 57.2±8.1ms, P < 0.001; FDG uptake: 63±12 versus 42±17, P < 0.001). All segments with no LGE showed complete recovery of wall motion at one year. There was no correlation between the wall motion score and FDG uptake in these later segments (R -0.06, P=0.82).

Among the segments with LGE, 34 segments (45%) had <50% transmural LGE and 41 segments (55%) had ≥50% transmural LGE with no difference in T2 values between these 2 groups (T2: 55.7±8.1ms versus 58.4±7.9ms, P=0.18). However, FDG uptake was significantly lower in segments with ≥50% transmural LGE (FDG uptake for LGE<50% 50±15 versus 35±16 for LGE>50%, P< 0.001) and these segments were also least likely to recover regional wall motion (LGE<50%: 27/34 – 79% recovered wall motion compared with LGE≥50% 20/41 – 49% recovered wall motion, P=0.006).

All segments with early MVO had ≥50% transmural LGE. When considering only segments with ≥50% transmural LGE, those with early MVO (n=20, 49%) had lower T2 values (consistent with intramyocardial hemorrhage - IMH) but similar level of FDG uptake compared with those without early MVO and these segments were also least likely to recover wall motion (T2: 55.4±5.9ms versus 62.0±8.6ms, P=0.01; FDG

uptake:  $31 \pm 14$  versus  $39 \pm 17$ ,  $P=0.09$ ; wall motion recovery: 5/20 – 25% for those with early MVO versus 15/21 for those without – 75%,  $P=0.004$ ).

ROC curve analysis showed acute LGE and FDG performed equally well (AUC 0.82, 95% CI 0.72 – 0.90 and 0.82, 95% CI 0.72 – 0.90,  $P=0.94$ ) but better than T2 (AUC 0.66, 95% CI 0.55 to 0.76,  $P=0.02$  and  $P=0.04$  respectively) to predict segmental wall motion recovery.

## **DISCUSSION**

Using hybrid cardiac PET-MR imaging in reperfused STEMI patients, we found that the area of reduced myocardial glucose uptake by FDG-PET imaging closely matched the AAR delineated by T2-mapping. In STEMI patients with minimal myocardial salvage the areas of reduced FDG uptake were confined to the areas of LGE, confirming that cardiac metabolism was impaired within the irreversibly injured myocardium within the MI. However, in patients with significant myocardial salvage the areas of reduced FDG uptake extended beyond the areas of LGE and closely matched the AAR delineated by T2-mapping. This demonstrates that in patients with significant myocardial salvage impaired cardiac metabolism was not confined to areas of irreversibly injured myocardium within the MI, but also included the reversibly injured salvaged myocardium within the AAR. In a subset of patients who had 12 month follow-up scans, the areas of reduced FDG uptake were significantly lower than those observed on the acute scans, and were now confined to the areas of LGE only. This demonstrates normalization of cardiac metabolism within reversibly injured salvaged myocardium in the AAR, leaving areas of reduced FDG uptake in irreversible (non-viable) tissue.

The reliable and accurate measurement of the AAR is required to assess myocardial salvage in clinical studies investigating novel cardioprotective interventions in reperfused STEMI patients. Cardiac MR allows the retrospective delineation of the AAR in STEMI patients treated by PPCI, and depends on the ability of T2-weighted and T2-mapping to delineate the extent of myocardial oedema within the AAR<sup>23</sup>. It has been validated by histology in animal MI models<sup>24, 25</sup>, and by angiography jeopardy scores<sup>26</sup> and myocardial SPECT imaging<sup>2, 27</sup> in STEMI patients. An alternative method to estimate the AAR is to measure the ESA of LGE<sup>19</sup>. However, unlike T2-weighted and T2-mapping, ESA is unable quantify the AAR in patients with minimal or absent infarction. Furthermore ESA has been shown to underestimate the AAR in STEMI patients when compared to T2-weighted imaging<sup>28</sup>. This finding was confirmed in a recent study<sup>11</sup>, in which the area of reduced FDG uptake was shown to over-estimate the AAR delineated by the ESA in reperfused STEMI patients.

There is currently no gold standard method for accurately quantifying the reduction in FDG uptake, and so we used manual delineation by 2 blinded operators as our reference standard, and compared it to 6 other established thresholding techniques. In this study, we found that a 2SD thresholding technique performed best for quantifying the areas of reduced myocardial glucose uptake. When using a threshold of 50% of peak – more conventional in the field of PET imaging – we found the limits of agreement between FDG-PET and T2 mapping were wide, likely due to the inherent differences in the 2 techniques used such as differences in spatial resolution and acquisition phase during the cardiac cycle.

The mechanism for the reduced FDG uptake observed in reversibly injured salvaged myocardium is not clear. Animal models have been used to elucidate the metabolic changes occurring in reversibly injured<sup>29, 30</sup> and stunned myocardium<sup>31-33</sup> but

due to the different ischemia/reperfusion protocols used and different baseline metabolic state of the animals prior to FDG administration, results from these studies regarding glucose and free fatty acid metabolism varied. However, putting these studies into context, it may be plausible that the reversibly injured but stunned myocardium preferentially uptakes more glucose than free fatty acid following a period of fasting compared to the normal myocardium but has delayed glucose metabolism. Therefore, after an oral glucose load, the reversibly injured myocardium has a reduced FDG uptake but subsequently normalizes on the follow-up scan.

Although a threshold of  $\geq 50\%$  of FDG uptake has been used to identify viable myocardium in the setting of stable coronary artery disease (CAD), the utility of FDG uptake in the acute setting has not been extensively studied. We have provided further insights into the definition and performance of LGE and FDG to detect viability in the acute setting, using the FDG uptake on the corresponding follow-up scan as gold standard. Shirasaki et al<sup>34</sup> has previously suggested a cut-off of 40% to detect viable myocardium, but FDG PET imaging was performed 2 weeks post AMI, and they used segmental wall motion recovery as the definition for viability. Rischpler et al<sup>8</sup> used a cut-off of  $\geq 50\%$  in the acute setting but no follow-up FDG PET was performed for comparison. Therefore our study is the first to provide validation of FDG uptake in the acute AMI setting by using follow-up FDG as the gold standard for viability.

We have also provided important insights into segmental wall motion recovery following AMI. Dysfunctional segments without LGE showed increased edema and reduced glucose metabolism yet recovered completely. Dysfunctional segments with early MVO showed evidence of intramyocardial hemorrhage (IMH) and reduced glucose metabolism and were least likely to recovery wall motion. Segments with predominantly reversibly injured myocardium were equally edematous compared to

segments with predominantly irreversibly injury myocardium but differed in glucose metabolism. T2 did not perform as well as LGE and FDG on the acute scan to predict functional recovery due to the paramagnetic properties of IMH reducing the T2 signal.<sup>35</sup> Despite only having a small number of segments without LGE but with wall motion abnormality, the lack of correlation between FDG uptake and wall motion score may be due to reduction in wall thickening giving rise to reduced FDG uptake appearance on the summed static FDG images.

#### *Limitations of study*

There were a number of exclusions in our study (diabetics, age <45 years old, previous MI, known contraindications for MR) and our findings are limited to a selected group of STEMI patients. Being a low volume PPCI center and compounded by the strict inclusion criteria, we managed to recruit a small number of patients. Follow-ups were performed in 12 patients only but these were sufficient to confirm recovery of FDG uptake in salvage myocardium. Current techniques for PET AC are known to increase image noise, cause image distortion and artifacts and therefore manual adjustment of copied endocardial and epicardial contours, assisted by visual optimization of window settings was required. The significant difference between the paired scans (acute and follow-up) in 12 patients supports the study findings of a reduction in FDG uptake in the AAR within a week of an acute STEMI. However, it is possible that by the use of summed static FDG-PET data, insufficient count recovery in stunned hypokinetic areas around the infarct border zone may have introduced an overestimation in the correlation between the FDG uptake and T2 mapping. The development of techniques for PET-MR cardiac phase registration, and partial volume correction, may improve future image analysis to confirm these findings.

### *Summary and conclusions*

We have demonstrated that the area of reduced myocardial glucose uptake in reversibly injured salvaged myocardium closely matched the AAR delineated by T2-mapping. Furthermore, FDG uptake, transmural extent of LGE and T2 values on the acute scan appear to predict subsequent myocardial viability and segmental wall motion recovery. With the advent of novel biological tracers, hybrid cardiac PET-MR has the potential to provide further insights into the pathophysiology of acute MI and subsequent post-MI LV remodeling.

### **ACKNOWLEDGEMENTS**

We express our gratitude to the staff and patients at the UCLH Heart Hospital. The investigational sequence for T2-mapping imaging was provided under a research collaboration agreement with Siemens Healthcare.

### **FUNDING**

This research study was funded by the British Heart Foundation (grant number FS/10/039/28270), the Rosetrees Trust, and was supported by the National Institute for Health Research University College London Hospitals Biomedical Research Centre. SKW is supported by British Heart Foundation Clinical Research Training Fellowship (grant number FS/10/72/28568).

### **DISCLOSURES**

None

## REFERENCES

1. Friedrich MG, Abdel-Aty H, Taylor A, Schulz-Menger J, Messroghli D and Dietz R. The salvaged area at risk in reperfused acute myocardial infarction as visualized by cardiovascular magnetic resonance. *Journal of the American College of Cardiology*. 2008;51:1581-7.
2. Carlsson M, Ubachs JF, Hedstrom E, Heiberg E, Jovinge S and Arheden H. Myocardium at risk after acute infarction in humans on cardiac magnetic resonance: quantitative assessment during follow-up and validation with single-photon emission computed tomography. *JACC Cardiovascular imaging*. 2009;2:569-76.
3. White SK, Hausenloy DJ and Moon JC. Imaging the myocardial microcirculation post-myocardial infarction. *Current heart failure reports*. 2012;9:282-92.
4. Betgem RP, de Waard GA, Nijveldt R, Beek AM, Escaned J and van Royen N. Intramyocardial haemorrhage after acute myocardial infarction. *Nature reviews Cardiology*. 2015;12:156-67.
5. Schlosser T, Nensa F, Mahabadi AA and Poeppel TD. Hybrid MRI/PET of the heart: a new complementary imaging technique for simultaneous acquisition of MRI and PET data. *Heart*. 2013;99:351-2.
6. Nensa F, Poeppel TD, Beiderwellen K, Schelhorn J, Mahabadi AA, Erbel R, Heusch P, Nassenstein K, Bockisch A, Forsting M and Schlosser T. Hybrid PET/MR imaging of the heart: feasibility and initial results. *Radiology*. 2013;268:366-73.
7. Rischpler C, Nekolla SG, Dregely I and Schwaiger M. Hybrid PET/MR imaging of the heart: potential, initial experiences, and future prospects. *Journal of nuclear medicine : official publication, Society of Nuclear Medicine*. 2013;54:402-15.
8. Rischpler C, Langwieser N, Souvatzoglou M, Batrice A, van Marwick S, Snajberk J, Ibrahim T, Laugwitz KL, Nekolla SG and Schwaiger M. PET/MRI early after myocardial infarction: evaluation of viability with late gadolinium enhancement transmural vs. <sup>18</sup>F-FDG uptake. *European heart journal cardiovascular Imaging*. 2015;16:661-9.
9. White SK, Frohlich GM, Sado DM, Maestrini V, Fontana M, Treibel TA, Tehrani S, Flett AS, Meier P, Ariti C, Davies JR, Moon JC, Yellon DM and Hausenloy DJ. Remote ischemic conditioning reduces myocardial infarct size and edema in patients with ST-segment elevation myocardial infarction. *JACC Cardiovascular interventions*. 2015;8:178-88.
10. Botker HE, Kaltoft AK, Pedersen SF and Kim WY. Measuring myocardial salvage. *Cardiovascular research*. 2012;94:266-75.
11. Nensa F, Poeppel T, Tezgah E, Heusch P, Nassenstein K, Mahabadi AA, Forsting M, Bockisch A, Erbel R, Heusch G and Schlosser T. Integrated FDG PET/MR Imaging for the Assessment of Myocardial Salvage in Reperfused Acute Myocardial Infarction. *Radiology*. 2015:140564.
12. Machac J, Bacharach SL, Bateman TM, Bax JJ, Beanlands R, Bengel F, Bergmann SR, Brunken RC, Case J, Delbeke D, DiCarli MF, Garcia EV, Goldstein RA, Gropler RJ, Travin M, Patterson R, Schelbert HR and Quality Assurance Committee of the American Society of Nuclear C. Positron emission tomography myocardial

- perfusion and glucose metabolism imaging. *Journal of nuclear cardiology : official publication of the American Society of Nuclear Cardiology*. 2006;13:e121-51.
13. Kramer CM, Barkhausen J, Flamm SD, Kim RJ, Nagel E and Society for Cardiovascular Magnetic Resonance Board of Trustees Task Force on Standardized P. Standardized cardiovascular magnetic resonance imaging (CMR) protocols, society for cardiovascular magnetic resonance: board of trustees task force on standardized protocols. *Journal of cardiovascular magnetic resonance : official journal of the Society for Cardiovascular Magnetic Resonance*. 2008;10:35.
  14. Giri S, Chung YC, Merchant A, Mihai G, Rajagopalan S, Raman SV and Simonetti OP. T2 quantification for improved detection of myocardial edema. *Journal of cardiovascular magnetic resonance : official journal of the Society for Cardiovascular Magnetic Resonance*. 2009;11:56.
  15. Martinez-Moller A, Souvatzoglou M, Delso G, Bundschuh RA, Cherdron C, Ziegler SI, Navab N, Schwaiger M and Nekolla SG. Tissue classification as a potential approach for attenuation correction in whole-body PET/MRI: evaluation with PET/CT data. *Journal of nuclear medicine : official publication, Society of Nuclear Medicine*. 2009;50:520-6.
  16. Baer FM, Voth E, Deutsch HJ, Schneider CA, Horst M, de Vivie ER, Schicha H, Erdmann E and Sechtem U. Predictive value of low dose dobutamine transesophageal echocardiography and fluorine-18 fluorodeoxyglucose positron emission tomography for recovery of regional left ventricular function after successful revascularization. *Journal of the American College of Cardiology*. 1996;28:60-9.
  17. Cerqueira MD, Weissman NJ, Dilsizian V, Jacobs AK, Kaul S, Laskey WK, Pennell DJ, Rumberger JA, Ryan T, Verani MS, American Heart Association Writing Group on Myocardial S and Registration for Cardiac I. Standardized myocardial segmentation and nomenclature for tomographic imaging of the heart. A statement for healthcare professionals from the Cardiac Imaging Committee of the Council on Clinical Cardiology of the American Heart Association. *The international journal of cardiovascular imaging*. 2002;18:539-42.
  18. Kim RJ, Wu E, Rafael A, Chen EL, Parker MA, Simonetti O, Klocke FJ, Bonow RO and Judd RM. The use of contrast-enhanced magnetic resonance imaging to identify reversible myocardial dysfunction. *The New England journal of medicine*. 2000;343:1445-53.
  19. Ortiz-Perez JT, Meyers SN, Lee DC, Kansal P, Klocke FJ, Holly TA, Davidson CJ, Bonow RO and Wu E. Angiographic estimates of myocardium at risk during acute myocardial infarction: validation study using cardiac magnetic resonance imaging. *European heart journal*. 2007;28:1750-8.
  20. Shrout PE and Fleiss JL. Intraclass correlations: uses in assessing rater reliability. *Psychol Bull*. 1979;86:420-8.
  21. DeLong ER, DeLong DM and Clarke-Pearson DL. Comparing the areas under two or more correlated receiver operating characteristic curves: a nonparametric approach. *Biometrics*. 1988;44:837-45.
  22. Hinkle DE, Wiersma W and Jurs SG. *Applied statistics for the behavioral sciences*. 4th ed. Boston: Houghton Mifflin Company; 1998.
  23. McAlindon EJ, Pufulete M, Harris JM, Lawton CB, Moon JC, Manghat N, Hamilton MC, Weale PJ and Bucciarelli-Ducci C. Measurement of myocardium at risk

- with cardiovascular MR: comparison of techniques for edema imaging. *Radiology*. 2015;275:61-70.
24. Aletras AH, Tilak GS, Natanzon A, Hsu LY, Gonzalez FM, Hoyt RF, Jr. and Arai AE. Retrospective determination of the area at risk for reperfused acute myocardial infarction with T2-weighted cardiac magnetic resonance imaging: histopathological and displacement encoding with stimulated echoes (DENSE) functional validations. *Circulation*. 2006;113:1865-70.
25. Ibanez B, Prat-Gonzalez S, Speidl WS, Vilahur G, Pinero A, Cimmino G, Garcia MJ, Fuster V, Sanz J and Badimon JJ. Early metoprolol administration before coronary reperfusion results in increased myocardial salvage: analysis of ischemic myocardium at risk using cardiac magnetic resonance. *Circulation*. 2007;115:2909-16.
26. Berry C, Kellman P, Mancini C, Chen MY, Bandettini WP, Lowrey T, Hsu LY, Aletras AH and Arai AE. Magnetic resonance imaging delineates the ischemic area at risk and myocardial salvage in patients with acute myocardial infarction. *Circulation Cardiovascular imaging*. 2010;3:527-35.
27. Langhans B, Nadjiri J, Jahnichen C, Kastrati A, Martinoff S and Hadamitzky M. Reproducibility of area at risk assessment in acute myocardial infarction by T1- and T2-mapping sequences in cardiac magnetic resonance imaging in comparison to Tc99m-sestamibi SPECT. *The international journal of cardiovascular imaging*. 2014;30:1357-63.
28. Fuernau G, Eitel I, Franke V, Hildebrandt L, Meissner J, de Waha S, Lurz P, Gutberlet M, Desch S, Schuler G and Thiele H. Myocardium at risk in ST-segment elevation myocardial infarction comparison of T2-weighted edema imaging with the MR-assessed endocardial surface area and validation against angiographic scoring. *JACC Cardiovascular imaging*. 2011;4:967-76.
29. Schwaiger M, Schelbert HR, Ellison D, Hansen H, Yeatman L, Vinten-Johansen J, Selin C, Barrio J and Phelps ME. Sustained regional abnormalities in cardiac metabolism after transient ischemia in the chronic dog model. *Journal of the American College of Cardiology*. 1985;6:336-47.
30. Buxton DB, Mody FV, Krivokapich J, Phelps ME and Schelbert HR. Quantitative assessment of prolonged metabolic abnormalities in reperfused canine myocardium. *Circulation*. 1992;85:1842-56.
31. McFalls EO, Baldwin D, Marx D, Fashingbauer P and Ward H. Temporal changes in function and regional glucose uptake within stunned porcine myocardium. *Journal of nuclear medicine : official publication, Society of Nuclear Medicine*. 1996;37:2006-10.
32. Hacker TA, Renstrom B, Nellis SH and Liedtke AJ. Effect of repetitive stunning on myocardial metabolism in pig hearts. *The American journal of physiology*. 1997;273:H1395-402.
33. Di Carli MF, Prcevski P, Singh TP, Janisse J, Ager J, Muzik O and Vander Heide R. Myocardial blood flow, function, and metabolism in repetitive stunning. *Journal of nuclear medicine : official publication, Society of Nuclear Medicine*. 2000;41:1227-34.
34. Shirasaki H, Nakano A, Uzui H, Yonekura Y, Okazawa H, Ueda T and Lee JD. Comparative assessment of 18F-fluorodeoxyglucose PET and 99mTc-tetrofosmin SPECT for the prediction of functional recovery in patients with reperfused acute myocardial infarction. *Eur J Nucl Med Mol Imaging*. 2006;33:879-86.

35. Wu KC. CMR of microvascular obstruction and hemorrhage in myocardial infarction. *Journal of cardiovascular magnetic resonance : official journal of the Society for Cardiovascular Magnetic Resonance*. 2012;14:68.

## Tables

**Table 1: Patients clinical characteristics and coronary angiographic details**

Details	Number
Number of patients	21
Male	16 (76%)
Age	59 ±10
Previous coronary artery disease*	2 (10%)
Hypertension	8 (38%)
Smoking	10 (48%)
Dyslipidemia	4 (19%)
Body Mass Index (kg/m <sup>2</sup> )	27.4±3.4
Chest pain onset to PPCI time (minutes)	247 [119-687]
Infarct artery (%)	
LAD	13 (62)
Proximal	6 (46)
Mid	6 (46)
Distal	1 (8)
RCA	8 (38)
Proximal	3 (37)
Mid	2 (25)
Distal	3(37)
Pre-PPCI TIMI flow (%)	
0	16 (76)
1	4 (19)
2	1 (5)
3	0 (0)
Post-PPCI TIMI flow (%)	
0	1 (5)
1	0 (0)
2	2 (9)
3	18 (86)

Number of vessels Single vessel disease Double vessel disease	16 (76) 5 (24)
AAR BARI score (% LV volume) APPROACH score (% LV volume)	28.7±8.3 29.4±9.8
Treatment – during PPCI Aspirin Clopidogrel Ticagrelor Prasugrel Heparin Bivalirudin Glycoprotein IIb/IIIa inhibitors Thrombectomy	21(100%) 1 (5%) 18 (86%) 2 (9%) 14 (67%) 14 (67%) 11 (52%) 17 (81%)
Treatment – on discharge Dual antiplatelet therapy Beta blockers ACEI/ARB Statin Mineralocorticoid receptor antagonist Warfarin (apical thrombus)	21(100%) 20(95%) 20(95%) 21(100%) 4(19%) 4 (19%)

LAD: left anterior descending artery; RCA: right coronary artery; TIMI: thrombolysis in myocardial infarction; LV: left ventricle; SD: standard deviation; AAR: area at risk; ACEI/ARB: angiotensin converting enzyme inhibitor/ angiotensin receptor blocker.

\*not previously known – subtotal occlusions of obtuse marginal branches in both cases and subendocardial infarct on MR, in the absence of edema.

**Table 2: Hybrid PET-MR findings on acute scan**

Characteristic	Number
Time from PPCI to hybrid PET-MR scan (days)	5 [4-6]
Left ventricular ejection fraction (%)	50±11 (Normal range 58-76)
End diastolic volume (ml)	138±22 (Normal range 113-196)
Left ventricular mass (g)	150±46 (Normal range 107-184)
Presence of MVO (%)	11 (46)
Presence of apical thrombus (%)	4 (19)
MI size by LGE MR (% LV volume)	22.3±11.7
AAR by T2-mapping MR (% LV volume)	36.3±12.2
AAR by FDG-PET (% LV volume)	37.2±11.6

Data are mean ± SD; PPCI: primary percutaneous coronary intervention; PET: positron emission tomography; MR: magnetic resonance; MVO: microvascular obstruction; MI: myocardial infarction; LGE: late gadolinium enhancement; AAR: area-at-risk; FDG: 18F-fluorodeoxyglucose

**Table 3: Quantifying the areas of reduced FDG uptake**

AAR by FDG-PET quantification		P value	ICC	Correlation (R value)	Bias±2SD
Manual	Other thresholds				
36.6±12.5	2SD: 37.2±11.6	0.07	0.99	0.99	-0.9±4.33
36.6±12.5	3SD: 24.2±13.0	0.001	0.49	0.46	12.9±20.0
36.6±12.5	4SD: 14.9±10.9	0.001	0.23	0.66	22.3±19.5
36.6±12.5	5SD: 7.8±7.3	0.001	0.10	0.55	29.4±20.7
36.6±12.5	FWHM: 38.5±19.2	0.61	0.74	0.80	-1.3±23.7
36.6±12.5	Otsu: 41.7±12.0	0.09	0.53	0.55	-4.5±23.3

AAR, area-at-risk; FDG-PET: 18F-fluorodeoxyglucose positron emission tomography. ICC intra-class coefficient

\*P values are for manual versus each threshold method

**Table 4: Hybrid PETMR findings in 12 patients with acute and follow-up scans**

	<b>Acute scan</b>	<b>Follow-up scan</b>	<b>P</b>
LVEF (%)	52 [47-59]	57 [47-68]	0.03*
End diastolic volume (ml)	147 [126-159]	152 [133-168]	0.33
Left ventricular mass (g)	150 [122-167]	110 [90-122]	0.002*
MI size (% LV volume)	27.7 [8.1-35.5]	19.0 [2.0-28.0]	0.005*
FDG-PET (% LV volume)	44.0 [21.3-55.3]	19.5 [6.3-31.8]	0.002*

Data are median [Interquartile range]. \* denotes statistical significance.

LVEF: left ventricular ejection fraction; MI: myocardial infarction; FDG-PET: 18F-fluorodeoxyglucose positron emission tomography.

## **Figures legend**

**Figure 1: The hybrid PET-MR cardiac imaging protocol**

(FDG:  $^{18}\text{F}$ -fluorodeoxyglucose; PET: Positron emission tomography; AC: Attenuation correction; EGE: Early gadolinium enhancement; LGE: Late gadolinium

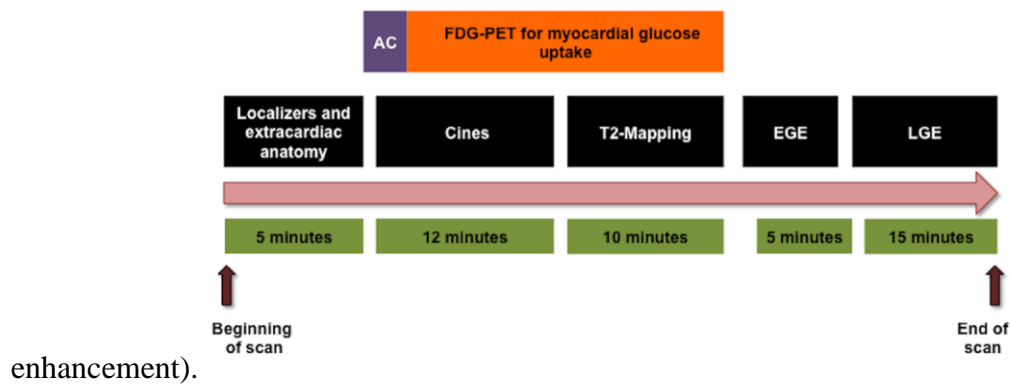
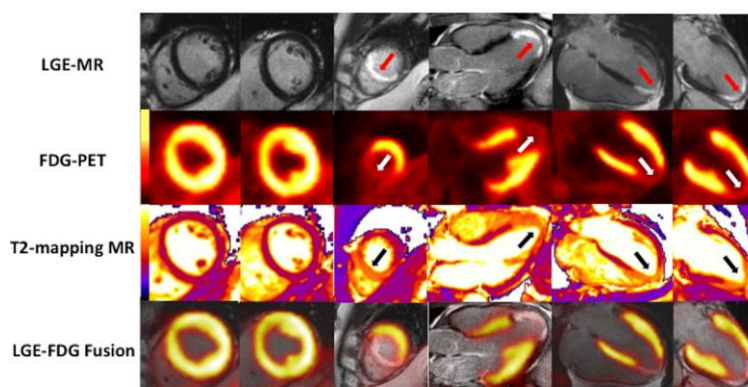


**Figure 2: Hybrid PET-MR cardiac imaging of transmural infarction**

A representative study patient with a distal LAD occlusion. Top panel: LGE-MR shows a transmural infarction confined to the LV apex and apical septum (red arrows); Upper middle panel: Corresponding FDG-PET images show areas of reduced FDG uptake matching those of infarction (white arrows); Lower middle panel: Corresponding T2 mapping MR images showing areas of increased T2 values matching the areas of reduced FDG uptake (black arrows); Bottom panel: Corresponding fused LGE-MR and FDG-PET images showing co-localization of the area of infarction and reduced FDG



uptake.

**Figure 3: Hybrid PET-MR cardiac imaging of subendocardial infarction**

Three study patients with subendocardial myocardial infarction (red arrows) with significant myocardial salvage. The areas of reduced FDG uptake (black arrows) and

the areas of edema on T2 maps (the AAR) (white arrows) extended both transmurally and radially beyond the areas of LGE.

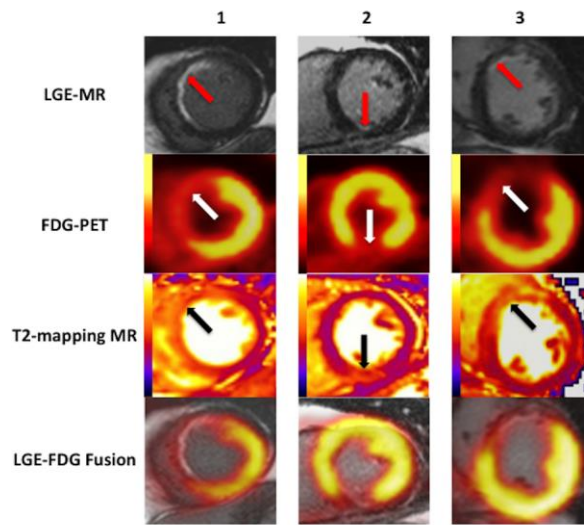


**Figure 4: Quantifying the area of reduced FDG uptake using different thresholding techniques**

\* denotes statistical significance.

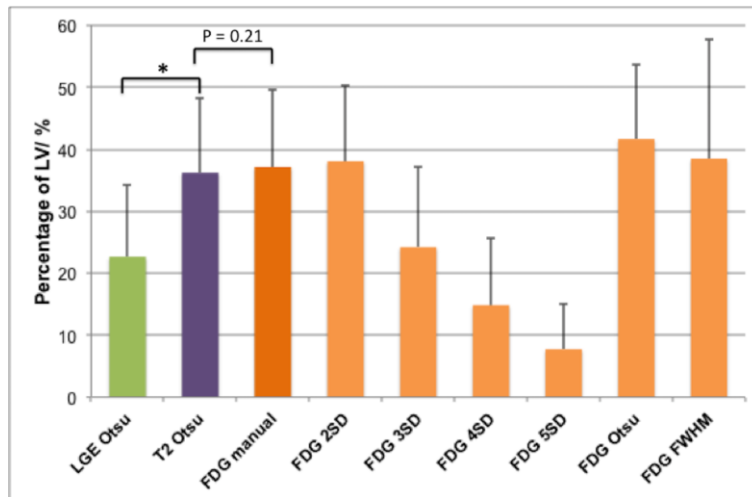


**Figure 5: Correlation and agreement between reduced FDG uptake and the AAR delineated by T2-mapping (a & b using 2SD for reduction in FDG uptake quantification and c & d using a threshold of 50% on the polar maps).**

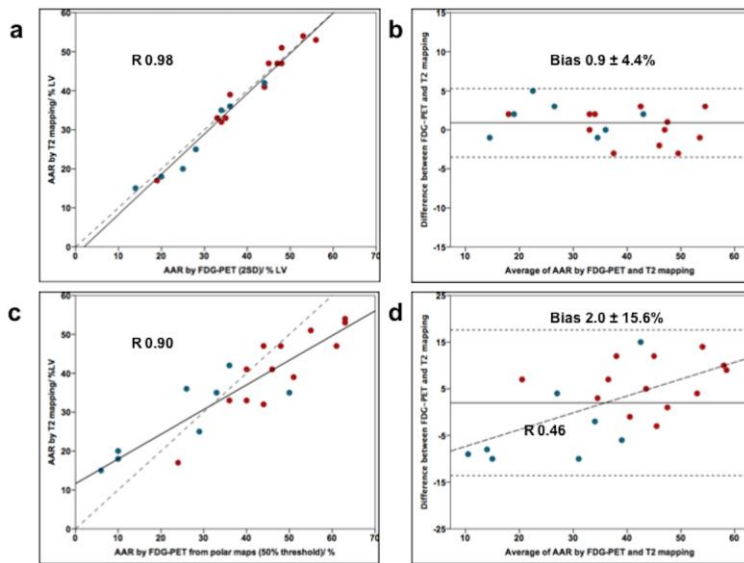


**Figure 6: Comparison of FDG uptake and LGE between the acute and 12 month follow-up hybrid cardiac PET-MR scans**

\* denotes statistical significance

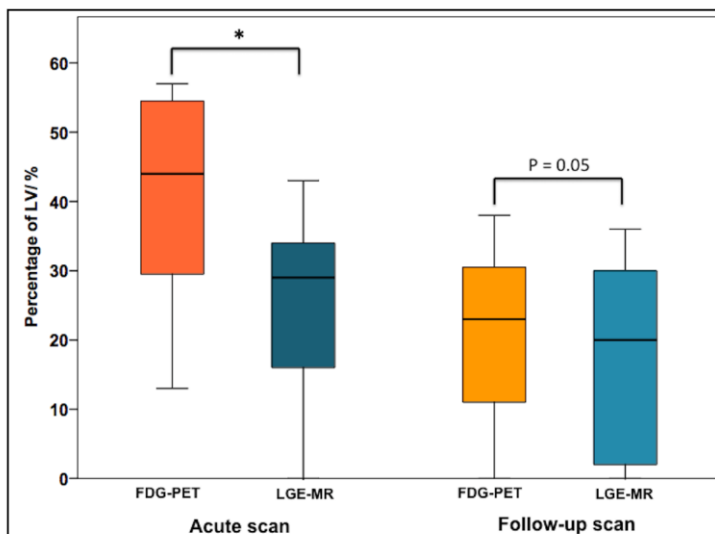


**Figure 7: FDG uptake in acute and follow-up hybrid cardiac PET-MR scans**

Representative LV short axis slices of FDG-PET and LGE-MR images in 2 STEMI patients with differing degrees of myocardial salvage. Patient A presented with an anterior STEMI and transmural myocardial infarction (red arrow) on the acute scan. On the follow-up scan there is no significant change in the area of reduced FDG uptake

confirming non-viable myocardium in the infarct zone. Patient B presented with an inferior subendocardial myocardial infarction (red arrow). The area of reduced FDG uptake is substantially larger than the area of LGE indicating significant myocardial salvage. On the follow-up scan there is a significant reduction in the area of reduced FDG uptake which is now restricted to the infarct zone.

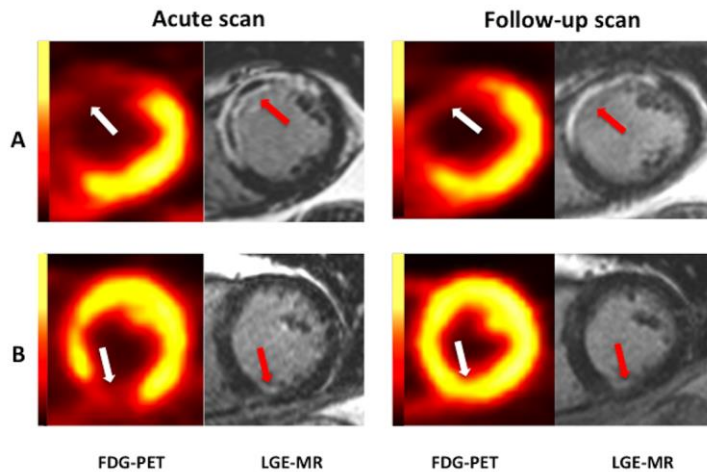
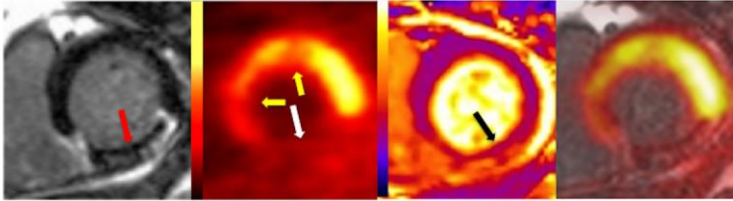


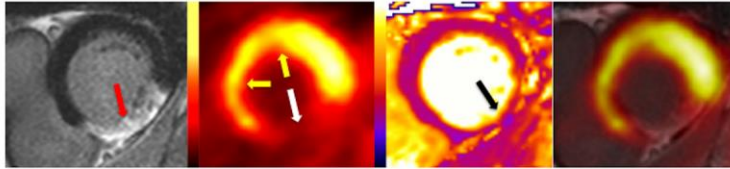
**Figure 8: Reduced myocardial glucose uptake in remote myocardium**

One study patient with a mid-right coronary artery STEMI had an area of reduced FDG uptake (white arrow) matching the inferior infarct by LGE (red arrow) and the AAR in the inferior LV wall by T2-mapping (black arrow). There was an additional area of reduced FDG uptake in the anterior and antero-septal walls (yellow arrows) in remote myocardium. The follow-up scan showed improvement in FDG uptake in the anterior and antero-septal walls of the remote myocardium.

Acute scan



Follow-up scan



LGE-MR

FDG-PET

T2-mapping MR

LGE-FDG Fusion